Journal of Solid State Chemistry 181 (2008) 2260–2267

Contents lists available at ScienceDirect

Journal of Solid State Chemistry

journal homepage: www.elsevier.com/locate/jssc

Polymorphism in $PbBiOXO_4$ compounds (X = V, P, As). Part I: Crystal structures of α- and β-$PbBiOVO_4$

Olfa Labidi [a], Pascal Roussel [a], Florence Porcher [b], Michel Drache [a,*], Rose-Noëlle Vannier [a], Jean-Pierre Wignacourt [a]

[a] Unité de Catalyse et de Chimie du Solide, CNRS UMR 8181 (Equipe de Chimie du Solide), ENSCL, USTL, 59655 VILLENEUVE D'ASCQ Cedex, France
[b] Laboratoire Léon Brillouin (LLB), CEA-CNRS UMR 12, CEA, Saclay, F 91191 Gif/Yvette, France

ARTICLE INFO

Article history:
Received 18 February 2008
Received in revised form
9 May 2008
Accepted 13 May 2008
Available online 23 May 2008

Keywords:
Phase transition
Mixed oxides
Twinned crystals
Neutron diffraction

ABSTRACT

Reinvestigation of $PbBiOVO_4$ thermal behaviour revealed a phase transition. As shown by single-crystal X-ray diffraction and high-resolution neutron powder diffraction, α-$PbBiOVO_4$ transforms to β-$PbBiOVO_4$ at 550 °C. At 25 °C, α-$PbBiOVO_4$ is triclinic, S.G. P-1, $Z = 2$, with $a = 5.6088(3)$, $b = 7.1109(3)$, $c = 7.2978(3)$ Å, $\alpha = 108.957(2)$, $\beta = 111.889(2)$, and $\gamma = 94.833(2)°$. Above 550 °C, β-$PbBiOVO_4$ is monoclinic, S.G. $C2/m$, $Z = 4$, with $a = 13.61(1)$, $b = 5.64(1)$, $c = 7.18(1)$ Å, and $\beta = 113.75(1)°$. Both structures are built upon $(O_2Bi_2Pb_2)_\infty$ chains parallel to the [100] direction in the α polymorph and [001] in the β-polymorph. These chains are undulated in α and linear in β. In both structures, VO_4 tetrahedra are organized in two sets of rows parallel to $(O_2Bi_2Pb_2)_\infty$ chains, thus building layers of (OBiPb) sandwiched by two layers of VO_4 oriented head to tail; VO_4 displays different orientations in α- and β-$PbBiOVO_4$.

1. Introduction

In a survey of nPbO–BiXO$_4$ (X = V, P, As) compounds, phases corresponding to $n = 1$, i.e., $PbBiOVO_4$, $PbBiOPO_4$ and $PbBiOAsO_4$, have been described [1–3].

$PbBiOVO_4$ was initially identified by Brixner [1]. It melts congruently at 895 °C. A yellow single crystal was grown from the Czochralski technique, and its structural study, using the precession method on films, revealed a triclinic symmetry with lattice parameters (a∼5.60 Å, b∼7.11 Å, c∼7.21 Å, α∼109°, β∼112°, γ∼95°, and V∼248 Å^3). Based on a negative second harmonic generation test, Brixner concluded the space group was P-1. No phase transition was reported.

In 1985, Wang and Li [4] reinvestigated the structure from a single-crystal study. In contrast to Brixner, the acentric distribution of the normalized structure factors oriented his choice towards the non-centrosymmetric space group, P1. The structure refinement yielded a final reliability factor of $R = 9.8\%$, with isotropic temperature factors, dropping to 7.9% while introducing anisotropic coefficients for heavy atoms. The Pauling's method (evaluation of bonding forces as a function of bond lengths) was applied for bismuth–lead identification. The final vanadium and oxygen thermal factors were either weak or negative. By careful examination of the atomic positions, Vannier [5] evidenced a symmetry relationship for heavy atoms positions, related two by two through a hypothetical centre of symmetry, located at 0.23, 0.46, and 0.43 implying that the real space group would be P-1. She carried out a thermodiffraction study, using a Guinier Lenné moving film camera, and evidenced a phase transition at 550 °C. This transition was not confirmed by differential thermal analysis (DTA) but a slight change of the thermal capacity was evidenced at 480 °C on heating and 450 °C on cooling by Differential Scanning Calorimetry, which was interpreted as a possible second-order phase transition. The refinement of the unit-cell parameters in function of the temperature evidenced a triclinic to monoclinic evolution. The high-temperature pattern could be indexed in a C centred unit cell with the lattice constants: a∼13.63 Å, b∼5.66 Å, $c = 7.20$ Å, and β∼114°. Single crystals were prepared but since they were systematically twinned, no further structural characterization was carried out at that time.

In the present study, a new approach to prepare $PbBiOVO_4$ single crystals was successfully conducted, allowing an X-ray single-crystal diffraction reinvestigation of the structural transformation. To obtain a more accurate location of oxygen atoms and discriminate bismuth and lead atoms ($b_{Pb} = 0.940 \times 10^{-12}$, $b_{Bi} = 0.885 \times 10^{-12}$, and $b_O = 0.580 \times 10^{-12}$ cm), high-resolution neutron powder diffraction was performed on the 3T2 diffractometer, at the Orphée Reactor of the Léon Brillouin Laboratory (LLB, Saclay, France), both at room (25 °C) and high (550 °C) temperatures.

* Corresponding author. Fax: +33 3 20 43 68 14.
E-mail address: michel.drache@ensc-lille.fr (M. Drache).

0022-4596/$ - see front matter © 2008 Elsevier Inc. All rights reserved.
doi:10.1016/j.jssc.2008.05.026

2. Experimental

2.1. Syntheses

$PbBiOVO_4$ powder samples were prepared by solid-state reaction of stoichiometric amounts of the starting reagents PbO (Riedel de Haën, 99%), Bi_2O_3 (Aldrich, 99.9%), and V_2O_5 (Aldrich, 99.6%). Compositions were weighed, mixed in an agate mortar, and fired at temperatures in the 600–800 °C range for a week, with intermediate grindings in order to obtain the desired single phase material.

A composition very slightly different from the nominal $PbBiOVO_4$ stoichiometry, i.e. 51.9% PbO, 22.2% Bi_2O_3, and 25.9% V_2O_5 (molar %) was also prepared. The powder sample was melted at 900 °C, followed by a recrystallization cooling process at 1 °C/h, until reaching 840 °C, at which temperature, the furnace was switched off until room temperature (RT). The selection of good-quality single crystals was based upon the definition and sharpness of their diffraction spots.

2.2. Characterization methods

Powder samples were characterized by RT X-ray diffraction, using a D8 Bruker diffractometer equipped with an energy dispersive point detector (SolX). The high-temperature X-ray diffraction patterns were, in a preliminary stage, measured using a Guinier Lenné diffraction camera with CuK_α radiation, in order to identify phase transitions. In a second stage, a D8 Bruker diffractometer equipped with an Anton Paar HTK1200N furnace and a Vantec1 linear detector was used in order to calculate the unit-cell parameters evolution as a function of temperature.

The powder samples thermal behaviour was also investigated by DTA on a Linseis L62 instrument, while dilatometry analysis was conducted on a Linseis L75 dilatometer. Both experiments were performed under air with a heating–cooling rate of 5 °C/min between RT and 700 °C.

RT single-crystal X-ray diffraction data were collected on a Bruker SMART APEX2 diffractometer (4K CCD detector). High-temperature single-crystal experiments were conducted on a Philips PW1100 diffractometer (point detector) equipped with an air flow heating device operating at 530 °C. For the two experiments, Mo$K\alpha$ radiation ($\lambda = 0.71073$ Å) was used. Experimental details are summarized in Tables 1 and 2.

Neutron powder diffraction experiments were performed on the high-resolution diffractometer 3T2 at the Orphée reactor at the Laboratoire Léon Brillouin (Saclay, France) with an incident neutron wavelength of 1.2265 Å. The powdered sample was introduced in a vanadium can, placed in a furnace for the data collection at 550 °C. The intensities were measured by a set of 20 ^{3}He counters. Full experimental details are given in Table 2.

3. Results and discussion

3.1. Identification of $PbBiOVO_4$ polymorphism

DTA was performed to characterize the thermal behaviour of $PbBiOVO_4$. However using this technique, no thermal effect was evidenced in its corresponding sub-solidus region.

The transition observed by Vannier [5], was confirmed by thermodiffraction between 450 and 500 °C (Fig. 1). The accuracy on the temperature measurement, which is better on the D8 diffractometer than on a Guinier Lenné system, was in good agreement with her DSC results. This evolution was identified as a triclinic–monoclinic phase transition.

The matrix relationship between the triclinic-α, and monoclinic-β cell is

$$\begin{pmatrix} a \\ b \\ c \end{pmatrix}_\beta = \begin{pmatrix} 1 & 0 & 2 \\ 1 & 0 & 0 \\ 0 & 1 & 0 \end{pmatrix} \begin{pmatrix} a \\ b \\ c \end{pmatrix}_\alpha$$

as represented in Fig. 2.

The evolution of the unit-cell volume versus temperature, calculated from the refined parameters, and the rapid decrease of the γ angle (triclinic setting) from 95.20 to 90°, characterize the phase transition (Fig. 3—top). This transition was also confirmed by a dilatometry study on a $PbBiOVO_4$ sintered pellet (Fig. 3—bottom): depending on the temperature, two linear domains were observed in good agreement with the volume evolution. Both techniques allow the determination of respectively the volume expansion coefficient and the linear expansion coefficient, below or above the transition identified nearby 500 °C. From the X-ray diffraction data, thermal volume expansion coefficients of $\alpha_\alpha \approx 35 \times 10^{-6}$ and $\alpha_\beta \approx 70 \times 10^{-6}\,K^{-1}$ were deduced in the α and β domains, respectively. Taking into account the obvious sintering completion of the pellet during its dilatometry investigation, the linear thermal expansion coefficients were estimated from the data on cooling: $\alpha_\alpha \approx 5 \times 10^{-6}$, $\alpha_\beta \approx 16 \times 10^{-6}\,K^{-1}$. These values are significantly different from the linear expansion coefficient calculated from the volume evolution (linear coefficient $\cong 1/3$ volume coefficient for isotropic structure); this observation is in good agreement with the anisotropy of α and β structures.

3.2. X-ray single-crystal data

3.2.1. α-$PbBiOVO_4$ structure at 25 °C

Needle-shaped crystals of α-$PbBiOVO_4$ were obtained and a first study suggested the presence of twinned entities, from the reciprocal lattice reconstruction, with lattice symmetry fitting to a monoclinic C lattice similar to the high-temperature form. A 180° rotation around the *a* cell parameter yielded a matrix relationship linking the two crystal components:

$$\begin{pmatrix} a \\ b \\ c \end{pmatrix}_{II} = \begin{pmatrix} 1 & 0 & 0 \\ -0.214 & -1 & 0 \\ -0.969 & 0 & -1 \end{pmatrix} \begin{pmatrix} a \\ b \\ c \end{pmatrix}_{I}.$$

In a different crystal sample, the twinning appeared to be identical, yielding a better structural refinement linked in this case to the predominance of one domain (twin ratio of 90.8%). This crystal was kept for structural investigation.

Data acquisition was conducted on a Bruker X8 CCD 4K diffractometer, using $K\alpha$ radiation of a molybdenum anode ($\lambda = 0.71073$ Å). Data collection and refinement conditions are summarized in Table 1. Reflection intensities of the two domains were extracted using the Saint 7.12 software, and TWINABS program [6] was used for absorption correction based on the redundancy [7] and for the creation of the different files used in the structural determination procedure. Intensities were flagged depending on the domain to which they belonged (domain 1, domain 2, or overlapping) and a so-called "HKLF5" dataset was created for the refinement. The crystal structure was solved on an "artificially untwined" so-called HKLF4 dataset (generated by TWINABS) in the *P*-1 centrosymmetric standard space group. Pb, Bi, and V heavy atoms were identified from direct methods with SIR97 [8], and oxygen atomic positions were obtained from Fourier Difference syntheses. JANA2006 (β version—2007) [9] was used for the final runs of the structural refinement using the HKLF5 dataset (i.e. with the whole dataset coming from domain 1, domain 2 and domain (1+2). Anisotropy was attributed to all

Table 1
Principal characteristics of $PbBiOVO_4$ X-ray diffraction single crystal and neutron powder structure determinations

Crystallographic data				
Radiation type	X-ray	Neutron	X-ray	Neutron
Chemical formula: $PbBiOVO_4$				
Formula weight (g): 547.1				
Temperature (°C)	25	25	530	550
Form	α	α	β	β
Symmetry	Triclinic	Triclinic	Monoclinic	Monoclinic
Space group	P-1 (No 2)	P-1 (No 2)	C2/m (No 12)	C2/m (No 12)
	$a = 5.6088(3)$	5.6089(1)	$a = 13.618(4)$	$a = 13.6269(1)$
	$b = 7.1109(3)$	7.1168(1)	$b = 5.635(2)$	$b = 5.649(6)$
	$C = 7.2978(3)$	7.3128(1)	$c = 7.184(2)$	$c = 7.1963(9)$
Cell parameters (Å, deg)	$\alpha = 108.957(2)$	109.07(2)	$\beta = 113.76(2)$	$\beta = 113.850(1)$
	$\beta = 111.889(2)$	111.857(2)	–	–
	$\gamma = 94.833(2)$	94.73(2)	–	–
Cell volume (Å^3)	248.33(2)	249.03(2)	504.5(2)	506.65(8)
Z	2	2	4	4
Density calculated (g cm^{-3})	7.30	7.29	7.20	7.17
F000	228	–	912	–
Data collection				
Diffractometer	Bruker X8	3T2 LLB Saclay	Philips PW1100	3T2 LLB Saclay
Monochromator	Graphite	Ge 335	Graphite	Ge 335
Detector	CCD 4K	20 3 He detectors	Point	20 3 He detectors
Wavelength radiation (Å)	0.71073 (Mo Kα)	1.22612	0.71073 (Mo Kα)	1.22612
2θ range (deg)	6.24–78.54	−5.38 to 121.92	6.20–59.96	−5.41 to 121.99
2θ step (deg)		0.05		0.05
Data collected	$-9 \leqslant h \leqslant 8$	–	$-18 \leqslant h \leqslant 16$	–
	$-12 \leqslant k \leqslant 11$	–	$-7 \leqslant k \leqslant 7$	–
	$-12 \leqslant l \leqslant 12$	–	$0 \leqslant l \leqslant 10$	–
No. of reflections collected	12026	–	1087	–
No. of reflections measured	2820	–	565	–
No. of independent ($I > 3\sigma(I)$)	2341	–	554	–
Redundancy	4.26	–	1.92	–
μ_1 mm^{-1} (Mo $K\alpha$)	72.2	–	72.2	–
$R(F^2)_{int}$	0.0493	–	0.0404	–
Refinement				
No. of parameters	75	63	32	38
Weighting scheme: $1/\sigma^2$				
$R(F)$ obs/all	0.0894/0.0977	–	0.1064/0.1224	–
w$R(F)$ obs/all	0.0646/0.0647	–	0.0520/0.0522	–
Second extinction	0.045(4)	–	–	–
Twin ratio	0.909(6)	–	0.77(3)	–
Background	–	10 Legendre polynomial terms combined with manual background	–	10 Legendre polynomial terms combined with manual background
R_p	–	0.0211	–	0.0223
wR_p	–	0.0274	–	0.0311
wR_{obs}	–	0.0187	–	0.0360
GOF	–	1.42	–	3.73
Analytical function for profile	–	Pseudo-Voigt	–	Pseudo-Voigt
Computer programs: Jana 2006—β version				

atoms in the last refinement cycles leading to satisfactory reliability factors (Table 1).

The neutron powder diffraction profiles were fitted using the Rietveld-type method implemented in the JANA2006 program. The observed profiles were described using a pseudo-Voigt profile shape function and the instrumental broadening respected the classical Caglioti function $(U\tan^2\theta + V\tan\theta + W)^{1/2}$, where U, V, and W are refinable parameters [10]. The background was adjusted using a 10-terms Legendre polynomial function. Systematic error corrections for zero-point and asymmetry were applied. The coherent scattering lengths used in the refinement were: $b_{Pb} = 0.940 \times 10^{-12}$, $b_{Bi} = 0.885 \times 10^{-12}$, and $b_O = 0.580 \times 10^{-12}$ cm. The starting crystallographic model was the refined structure from X-ray data out of the twinned single crystal. The vanadium atom was fixed at the position obtained from X-ray data, since V is invisible to neutron radiation. For each atom, anisotropic mean-square atomic displacements were considered in the last stage of the refinement. In a first step, tests for $P1$ space group instead of P-1 were performed. As they were not conclusive, the centrosymmetric space group was kept. In a second step, the positions of bismuth and lead atoms were tested. The previous assignment of Pb and Bi sites using the Pauling's rules was unambiguously confirmed by the agreement factors obtained for the two different possibilities ($R_{obs} = 1.68$, GOF = 1.52, $R_{wp} = 2.87$ for the "wrong" model compared to $R_{obs} = 1.52$, GOF = 1.45, $R_{wp} = 2.74$ for the "good" one). All details containing experimental set-up as well as refinement results are gathered in Table 1. Coordinates, equivalent and anisotropic displacement parameters (Å^2) of Pb, Bi, V, and O atoms are reported in Table 2.

Fig. 4a shows the observed and calculated neutron powder diffraction profiles at RT.

The structure of α-$PbBiOVO_4$ is given in Fig. 5. It shows that O2 atoms are located at the centre of OBi_2Pb_2 cationic tetrahedra built from Pb and Bi atoms, sharing Bi–Bi and Pb–Pb opposite edges, thus developing (OBiPb) infinite chains in the [100] crystallographic direction. Each of these $(OBiPb)_\infty$ chains is

Table 2
Coordinates, equivalent and anisotropic displacement parameters (Å^2) of Pb, Bi, V, and O atoms determined from neutron diffraction data for α- and β-$PbBiOVO_4$

Atom	x	y	z	U_{eq}	U_{11}	U_{22}	U_{33}	U_{12}	U_{13}	U_{23}
α-$PbBiOVO_4$ (25 °C)										
Pb1	0.6168(3)	0.8028(3)	0.1773(4)	0.0261(9)	0.0224(11)	0.0304(12)	0.0222(12)	0.0062(9)	0.0046(9)	0.0113(10)
Bi1	0.7664(3)	0.5321(3)	0.5658(4)	0.0125(8)	0.0121(9)	0.0090(10)	0.0123(10)	0.0010(9)	0.0010(8)	0.0033(9)
V1[a]	0.1545	−0.1518	0.1648	0.01	0.009998	0.010001	0.009999	0.003863	0.002328	0.004237
O1	0.2016(5)	0.1138(4)	0.3480(7)	0.0367(16)	0.033(2)	0.0114(16)	0.051(2)	0.0057(15)	−0.0102(17)	0.0051(16)
O2	0.1042(4)	0.3046(5)	−0.0773(6)	0.0275(14)	0.0181(17)	0.0188(16)	0.029(2)	−0.0044(14)	0.0003(13)	0.0037(15)
O3	0.7034(4)	0.2166(5)	0.6418(6)	0.0224(14)	0.0236(19)	0.0142(15)	0.0217(17)	0.0020(14)	0.0019(14)	0.0056(12)
O4	0.7541(5)	0.1872(5)	0.1086(7)	0.0341(17)	0.036(2)	0.049(2)	0.0224(18)	0.0163(18)	0.0179(16)	0.0184(16)
O5	0.5045(4)	0.4850(5)	0.2506(6)	0.0168(13)	0.0137(14)	0.0238(17)	0.0118(16)	0.0054(13)	0.0025(13)	0.0082(16)
β-$PbBiOVO_4$ (550 °C)										
Pb1	0.1533(5)	0	0.1042(10)	0.088(3)	0.085(5)	0.037(4)	0.118(5)	0	0.017(3)	0
Bi1	0.0236(4)	−0.5	0.2703(8)	0.056(3)	0.026(3)	0.094(5)	0.042(3)	0	0.008(3)	0
V1[a]	0.1715	0	0.65	0.028229	0.011163	0.036925	0.033479	0	0.005799	0
O1	0.0994(7)	0	0.3839(10)	0.122(6)	0.074(8)	0.250(12)	0.024(5)	0	0.000(6)	0
O2	0.1404(6)	0.2363(13)	0.7449(13)	0.118(4)	0.148(7)	0.074(5)	0.129(6)	−0.019(4)	0.054(5)	−0.032(4)
O3	0.1965(6)	−0.5	0.2829(13)	0.113(6)	0.031(6)	0.187(11)	0.119(8)	0	0.029(6)	0
O4	0	−0.2492(15)	0	0.054(4)	0.075(6)	0.059(5)	0.015(3)	0	0.005(4)	0

[a] Fixed at the positions refined from X-ray data.

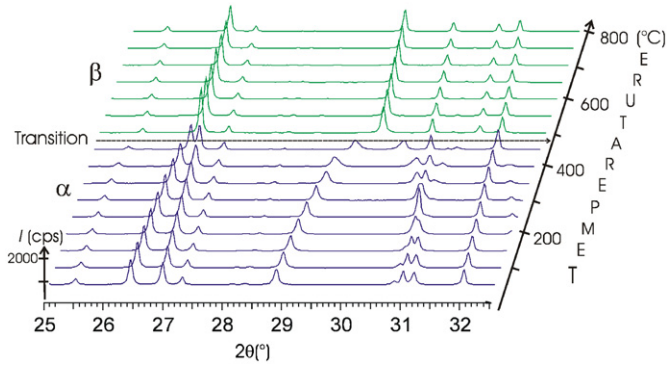

Fig. 1. $BiPbOVO_4$ X-ray thermodiffraction patterns.

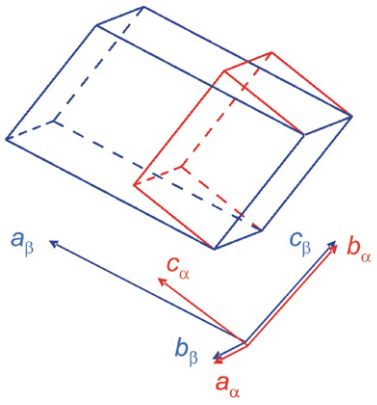

Fig. 2. Relationships between triclinic α-$PbBiOVO_4$, and monoclinic β-$PbBiOVO_4$ unit cells.

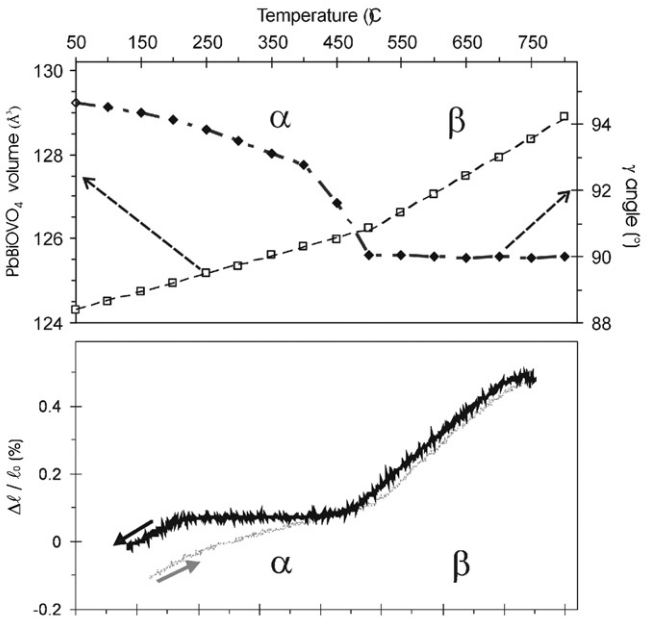

Fig. 3. Identification of α-/β-$PbBiOVO_4$ dimorphism from powder high-temperature X-ray diffraction (top) and dilatometry study of sintered pellet (bottom).

surrounded by two sets of 3 VO_4, A two-dimensional description can be seen with a layer of $(OBiPb)_\infty$ chains sandwiched by two layers of vanadate rows, parallel to the $(010)_\alpha$ plane, e.g., then designing a slab; the α-$PbBiOVO_4$ structure is thus obtained from a stacking of such slabs along $\vec{b}_\alpha$.

Bismuth (III) and lead (II) display of $6s^2$ lone pair in their electronic structure, which is known as a positive factor for enhancing polarization in the crystal structure, but also as a key factor for ionic migration within the material structure. The lone pair phenomenon is found in crystalline solids including in their formula heavy cations of the *p* bloc with an $ns^2\ np^0$ external electronic configuration, such as Sn^{2+}, Sb^{3+}, Pb^{2+}, Bi^{3+}, etc. Electrostatic repulsions resulting from the anionic surrounding on the s^2 atomic orbital, which is rather big and potentially polarizable, do not permit the building of any regular coordination polyhedra: a structural stabilization is achieved through a partial hybridization of the *ns* orbitals with vacant *np* levels. The so-called lone pair or non-bonding pair, can be identified, and approximately occupies a volume identical to an F^- or O^{2-} anion. It is located close to the anionic polyhedron centre, i.e. the cation core, and as a result, the internal orbitals are out-centred. This position is barely observed in a diffraction experiment because of its low electron density while compared to heavy atoms. Thus, the lone pair position of bismuth and lead atoms has been evaluated

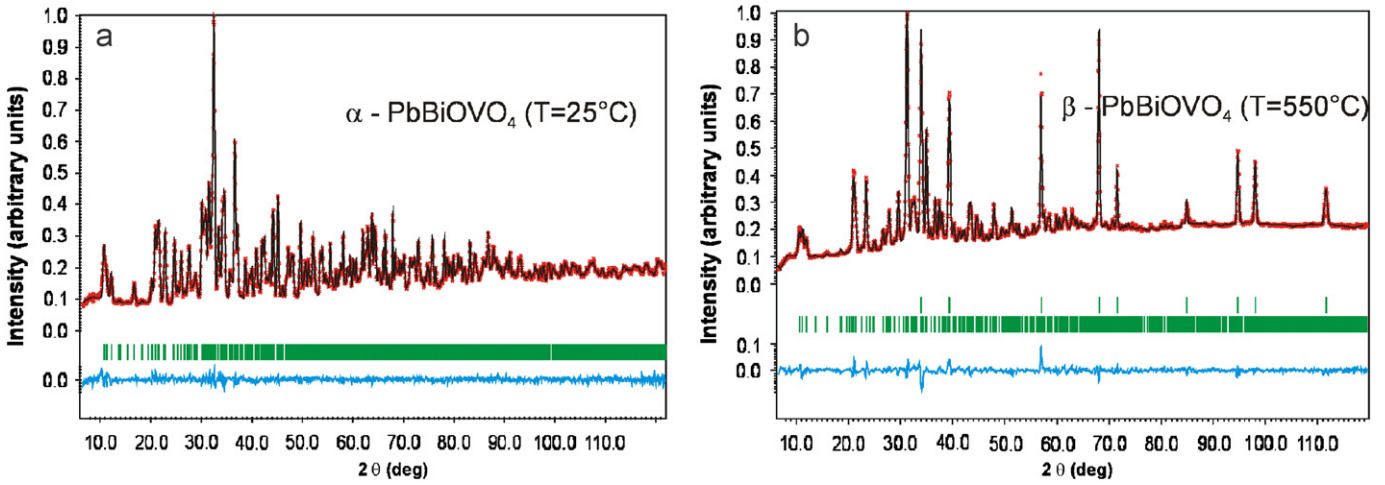

Fig. 4. $PbBiOVO_4$ powder neutron diffraction patterns observed (points) or calculated (continuous line), and difference between the observed and calculated patterns (lower part) for (a) α-form at 25 °C; (b) β-form at 550 °C.

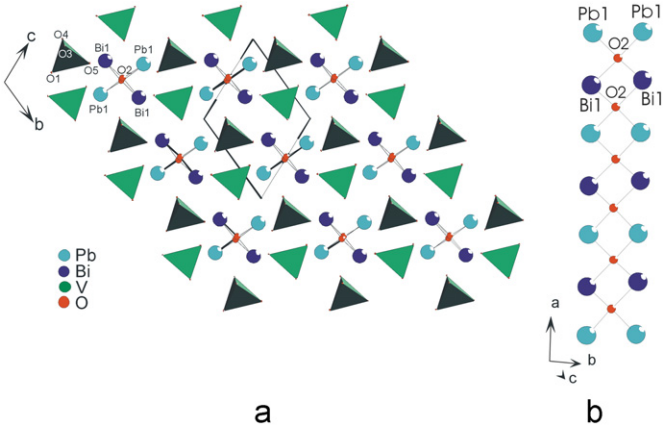

Fig. 5. α-$PbBiOVO_4$ structure viewed along [100] (a); $(OBiPb)_\infty$ chain ∥ *a* axis (b).

using a local modification of the program HYBRIDE, initially developed by Morin et al. [11]. In this approach, proposed by Verbaere et al. [12], the calculation is based upon electrostatic interactions between the core and the lone pair, leading to the basic formula of the induced polarization *P*, i.e. $P = -2d = \alpha E$, where −2 represents the charge of the lone pair, *d* the core–lone-pair distance, α the polarizability of the considered atom, and *E* the local electrostatic field calculated by Ewald's method [13]. According to Shannon [14], polarizability of lead and bismuth atoms are respectively 6.58 and 6.12 $Å^3$. However, as $PbBiOVO_4$ cannot be considered as purely ionic, we considered formal atom partial charges instead of oxidation states. The ionicity ratio of each bond was calculated using Pauling's formula [15], from the electronegativity difference taken from Zhang [16] and then applied to the cation oxidation states, giving charges of +1.23, +1.73, and +3.25, for Pb, Bi, and V atoms, respectively. Consequently, oxygen anions were given a balancing charge of −1.24. Calculations reached self-consistent positions for the 15 atoms of the structure. The lone pair positions and distances from nuclei are given in Table 3.

The Pb1 coordination polyhedron has a O2O3O4O2 distorted rectangular basis; plus 4 oxygen atoms O1, O5, O4, and O3, belonging to three different $V1O_4$ tetrahedra: O4 and O3 are from a single VO_4, O1 is from a second vanadate, which is implied by its O4 atom in the definition of the pseudo-rectangular basis, and O5 originates from a third tetrahedron. In that

Table 3
Lone pair positions and distances from nuclei (Å) in RT-$PbBiOVO_4$ (α), high-temperature $PbBiOVO_4$ (β)

Atom	*x*	*y*	*z*	$d_{nucleus}$–*L* (Å)
α-PbBiOVO₄ (T = 25 °C)				
Pb1	0.203	0.134	0.872	0.437
Bi1	0.576	0.348	0.565	0.551
β-PbBiOVO₄ (T = 530 °C)				
Pb1	0.306	0.000	0.856	0.519
Bi1	0.050	0.001	0.356	0.611

configuration, the Pb lone pair is directed towards the pseudo-rectangular basis, more specifically towards O4 and O3 atoms, as displayed in Figs. 5a–b. Bi1 coordination polyhedron looks alike an octahedron, built from a distorted O2O4O3O2 square base, with two O1 and O5 "apical" oxygen atoms from 2 independent tetrahedra, with O1 in axial position, but O5 being away from the 6th apex of the pseudo-octahedron, thus leaving space for the Bi lone pair.

3.2.2. *β-PbBiOVO₄ at 550 °C*

The high-temperature single-crystal data were collected on a Philips PW 1100 diffractometer equipped with a molybdenum anode ($\lambda MoK\alpha = 0.71073$ Å), a graphite monochromator, and an air flow heating device. The selected crystal was mounted in an amorphous silica capillary, and data were collected at 530 °C. While yellow at RT, the crystal turned deep orange at high temperature; this colour evolution was also noted while heating under a polarized light source. A monoclinic C centred unit cell was identified for the high-temperature form with $a = 13.618$ Å, $b = 5.635$ Å, $c = 7.184$ Å, and $\beta = 113.76°$, but many other reflections violating this cell were also observed. They were attributed to a twin, described in detail later. Hoping for a hypothetic "untwining" of the crystal, a number of heating/cooling runs were realized over a temperature range including the transition temperature. Despite many trials, and a final annealing treatment at 450 °C for 2 h, the sampled crystals remained twinned, making difficult the complete structural elucidation of the transition process, since our heating device is installed on a diffractometer equipped with a point detector.

The twinning scheme has been identified with a major component (twin ratio of 77%), from which the second one is

identified through a 180° rotation around the *a* lattice parameter. The matrix twinning operator is

$$\begin{pmatrix} a \\ b \\ c \end{pmatrix}_{II} = \begin{pmatrix} 1 & 0 & 0 \\ 0 & -1 & 0 \\ 1.527 & 0 & -1 \end{pmatrix} \begin{pmatrix} a \\ b \\ c \end{pmatrix}_{I}.$$

This twin is well imaged on the (*h0l*) layer (Fig. 6a), which displays the superposition of the two domains along the underlined direction. On the successive representation of the *hk*3 and *hk*4 levels, Figs. 6b and c, it is visible that the reflections of domain 1 and 2 coincide almost perfectly every 4*n* (*n* integer—Fig. 6c), while they are almost completely separated elsewhere (Fig. 6b).

As already pointed out, the PW1100 diffractometer is equipped with a point detector and the integration process cannot take into account the two domains simultaneously. Unfortunately, it was therefore impossible to generate an HKLF5 file as it was done for the RT form. However, the collected data were treated with JANA2006, a program which also takes into account the twinning function in a different way, i.e., calculating for all the reflections the difference between the position in the first domain and in the second domain (note that in this case, we have to assume that the reflections are either fully overlapped or fully separated). If the angular difference between the reflections belonging to the two domains is equal or smaller than the so-called "overlapping" parameter, the reflections are considered to be completely overlapped and the measured intensity is then $F^2(H) = v_1F^2(HT_1)+v_2F^2(HT_2)$ where v_i is the volume fraction of *i*th domain (the twin ratio) and T_i is the matrix representation of *i*th twinning operator. In the present case, T_1 is the identity matrix and T_2 the matrix given above. If now the angular difference between HT_1 and HT_2 is higher than the "overlapping parameter", the reflections are considered as completely separated, i.e. the measured intensity is only due to the domain 1. The best fit was obtained for the value 0.15°. This procedure allowed a rather good description of the *HT* form, which was lately completely confirmed by *HT* high-resolution neutron powder diffraction. The main structural results concerning the single-crystal X-ray determination of the β-$PbBiOVO_4$ form are given in Tables 1 and 2.

The high-resolution neutron data collected at 550 °C were used to confirm the model obtained on the twinned crystal. The powder was introduced in a vanadium container, placed in a furnace and heated under vacuum. Beside the β form of $PbBiOVO_4$, a second phase was introduced in the Rietveld procedure to account for the copper heating element of the furnace. All atoms with anisotropic atomic displacement parameters were refined with the JANA2006 program in the last cycles of the refinement. All details containing experimental set-up and refinement results are gathered in Tables 1 and 2. Fig. 4b shows the observed and calculated neutron powder diffraction profiles at high temperature.

The structure of β-$PbBiOVO_4$ shows infinite OBi_2Pb_2 chains along the [010] crystallographic direction. They are surrounded by six VO_4 tetrahedra organized in two sets with different configurations. A "slab" organization results from one layer of (OBi_2Pb_2) in between two layers of VO_4; the β-$PbBiOVO_4$ structure is obtained by stacking e.g. along c_β of such slabs, thus parallel to $(001)_\beta$, where every vanadate tetrahedron has a face parallel to these $(001)_\beta$ planes (Fig. 7).

The lone pair localization was calculated as described for the RT variety of $PbBiOVO_4$. Lone pair positions from the core, consequently determined for lead and bismuth, are reported in Table 2 and presented in Fig. 8.

The Pb1 coordination polyhedron displays a distorted rectangular basis built from O2O4O2O4 atoms, completed with three others belonging to three VO_4 tetrahedra: two O3, and O1 originating from a last and distinct VO_4. The Pb lone pair is pointing towards the missing corner of a pseudo-square face O1–O3–O3–L, opposite to the previously described one. The Bi1 polyhedron is described by four oxygen atoms O2O4O4O2 forming a slightly distorted square; the other oxygen atoms: 2 O1 and O3 are part of independent tetrahedra. The Bi lone pair L is oriented opposite to the square basis, towards the missing corner of a pseudo-cubic environment.

The structure of β-$PbBiOVO_4$ is analogous to the structure of $MgBiVO_5$ [17], described with infinite OBi_2Mg_2 chains and VO_4 groups along the [001] crystallographic direction. β-$PbBiOVO_4$ structure can be compared to Pb_2XO_5 (X = S, Cr, Mo) structures, solved from combined X-ray and neutron powder experiments at 5 K [18,19], in a monoclinic system, space group $C2/m$. The Pb_2SO_5 structure displays infinite (OPb_4) chains parallel to the [010]

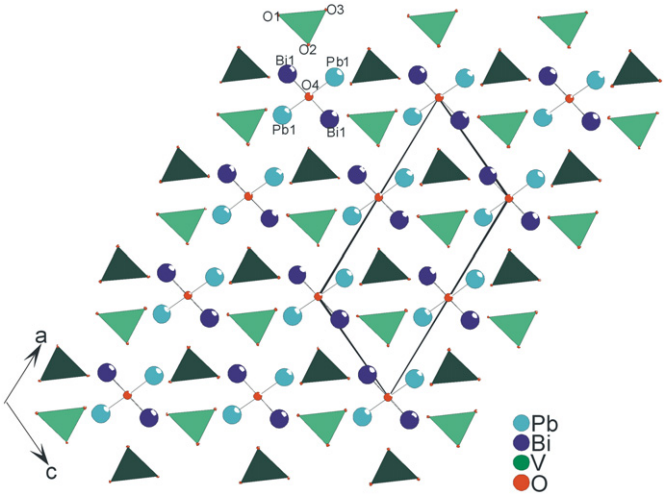

Fig. 7. β-$PbBiOVO_4$ at 530 °C, viewed along [010].

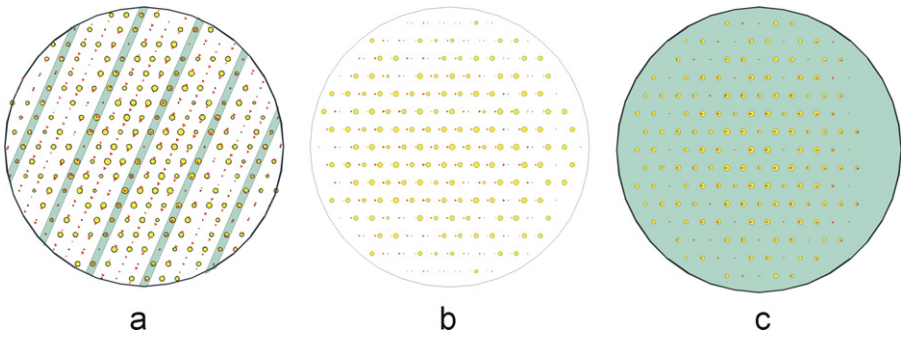

Fig. 6. Projections of *h0l* (a), *hk3* (b), and *hk4* (c) layers of the reciprocal space.

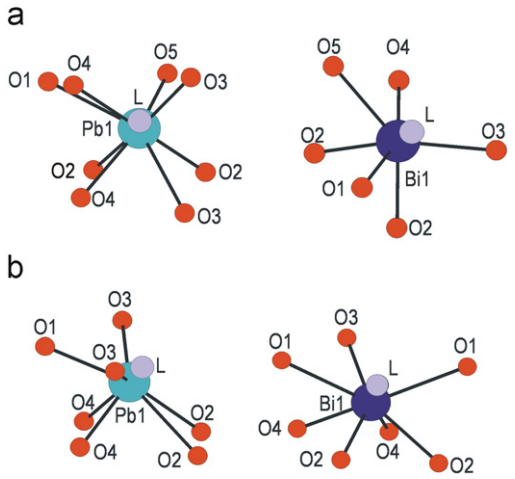

Fig. 8. Lone pair localization and oxygen environment of Pb and Bi atoms for (a) α-$PbBiOVO_4$ and (b) β-$PbBiOVO_4$.

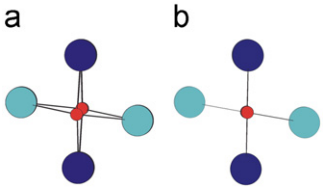

Fig. 9. $(OPb_2Bi_2)_\infty$ chain viewed in the direction (a) $\vec{a}_\alpha$(α-$PbBiOVO_4$) and (b) $\vec{b}_\beta$ (β-$PbBiOVO_4$).

crystallographic direction, linked to each other through (SO_4) tetrahedra, and Pb–O–S bridges. Wang and Li [4] proposed a comparison between Pb_2SO_5 and the $PbBiOVO_4$ triclinic configuration, suggesting that heavy atoms in both compounds are equivalent while shifting the origin at $x=-0.27$, $y=-0.04$, and $z=-0.60$. The tetrahedra orientation, i.e. XO_4 and VO_4, is identical in Pb_2XO_5 (X = S, Cr, Mo) and $PbBiOVO_4$ structures at 530 °C (Fig. 7).

3.2.3. *Low-temperature–high temperature structural evolutions*

The structural comparison of the low-temperature and high-temperature $PbBiOVO_4$ crystallographic forms shows several evolutions through the transition process which concern, at first, the $(OBi_2Pb_2)_\infty$ chains, backbone of the structure. In the low temperature α form, Fig. 9a, different bond lengths O2–Bi, as well as O2–Pb, are alternating; consequently, the resulting OBi_2Pb_2 tetrahedron is distorted, which produces an undulation within the $(OBi_2Pb_2)_\infty$ chain oriented along the direction of the crystallographic axis $a_\alpha = 5.6$ Å. In the high-temperature β form, the infinite chains are built from OBi_2Pb_2 tetrahedra, with rigorously identical distances O–Bi on one side, and O–Pb on the other, which are linked through common edges Pb–Pb and Bi–Bi alternatively, thus conferring a rigorously linear chain organization parallel to the crystallographic axis $b_\beta = 5.6$ Å (Fig. 9b).

Moreover, in the triclinic α-$PbBiOVO_4$, the VO_4 tetrahedra are organized in rows parallel to a_α, in two sets of crystallographically independent entities, while in the monoclinic β form, these rows of VO_4 tetrahedra, identified parallel to the b_β axis of the unit cell, display a specific orientation with their O2–O3–O2 faces parallel to the (001) crystallographic planes, and their O2–O1–O2 faces parallel to (100) planes, respectively.

As a conclusion, this reading of the high-temperature β-$PbBiOVO_4$ form shows an overall structural organization in alternating layers parallel to (001) planes with:

- a layer of independent $(OBi_2Pb_2)_\infty$ chains, oriented in the [010] direction; its central part is composed of oxygen atoms, sandwiched by Bi and Pb atoms laterally.
- a layer of double rows of VO_4 tetrahedra, oriented head to tail.

4. Conclusion

This reinvestigation of $PbBiOVO_4$ revealed a phase transition. Single-crystal X-ray diffraction and high-resolution neutron powder diffraction showed that α-$PbBiOVO_4$ (triclinic, P-1) transforms to β-$PbBiOVO_4$ (monoclinic, $C2/m$) at 550 °C, through a drastic evolution of their diffraction patterns. Both structures are built upon $(O_2Bi_2Pb_2)_\infty$ chains parallel to [100] in the α polymorph and [010] in the β-polymorph, a common lattice dimension that can be related to a Fluorite-type unit cell. These chains are undulated in α and linear in β. In both structures, VO_4 tetrahedra are organized in two sets of rows parallel to $(O_2Bi_2Pb_2)_\infty$ chains, thus building layers of OBiPb sandwiched by two layers of VO_4 oriented head to tail, where VO_4 displays different orientations in α- and β-polymorphs.

5. Supplementary materials

Crystal structure data, gathered in Tables 1 and 2, have been sent to the Fachinformationzentrum Karlsruhe, 76344 Eggenstein-Leopoldshafen, Germany (fax: (+49)7247-808-666; e-mail: crystaldata@fiz-karlsruhe.de; http://www.fiz-karlsruhe.de, as supplementary material CSD Nos. 419121 (for PbBiOVO4-RT-XC (RT structure of $PbBiOVO_4$ determined on single crystal using X-ray diffraction)), 419122 (PbBiOVO4-HT-NP (high temperature structure determined on powder using neutron diffraction)), 419123 (PbBiOVO4-HT-XC), 419126 (PbBiOVO4-RT-NP). Copies of this information can be obtained by contacting the FIZ (quoting the article details and the corresponding CSD number).

Acknowledgements

The Laboratoire Léon Brillouin (LLB) is thanked for providing neutron facilities. The "Fonds Européen de Développement Régional (FEDER)", "CNRS", "Région Nord Pas-de-Calais" and "Ministère de l'Education Nationale de l'Enseignement Supérieur et de la Recherche" are acknowledged for fundings of X-ray diffractometers. The authors are also grateful to P. Conflant and G. Nowogrocki for their Guinier Lenné investigation and interpretation, and to F. Bourrée (LLB) for the neutron data collection on powder samples. Dr. V. Petricek is also thanked for providing us the β-version of JANA2006.

References

[1] L.H. Brixner, C.M. Foris, MaterRes. Bull. 9 (1974) 273–276.
[2] S. Giraud, P. Conflant, M. Drache, J.P. Wignacourt, H. Steinfink, Phosphorus Res. Bull. 10 (1999) 138–143.
[3] S. Giraud, M. Mizrahi, M. Drache, P. Conflant, J.P. Wignacourt, H. Steinfink, Solid State Sci. 3 (2001) 593–602.
[4] P.-L. Wang, D.-Y. Li, Acta Phys. Sin. 34 (1985) 235–240.
[5] R.-N. Vannier, Thesis of Lille University, 1992.
[6] Bruker Analytical X-ray system, SAINT+, Version 7.12, Madison, USA, 2004.
[7] G.M. Sheldrick, SADABS, Bruker–Siemens Area Detector Absorption and Other Correction, Version 2006/1, 2006.

[8] A. Altomare, G. Cascarano, C. Giacovazzo, A. Guagliardi, "SIR 97," J. Appl. Crystallogr. 27 (1994) 1045–1050.
[9] V. Petricek, M. Dusek, L. Palatinus, JANA2006-β version, Institute of Physics, Praha, Czech Republic, 2007.
[10] C. Caglioti, A. Paoletti, E.P. Ricci, Nucl Instrum. Methods 3 (1958) 223.
[11] E. Morin, G. Wallez, S. Jaulmes, J.C. Couturier, M. Quarton, J. Solid State Chem. 137 (1998) 283–288.
[12] A. Verbaere, R. Marchand, M. Tournoux, J. Solid State Chem. 23 (1978) 383–390.
[13] P.P. Ewald, Ann. Phys. 64 (1921) 253–287.
[14] R.D. Shannon, J. Appl. Phys. 73 (1993) 348–366.
[15] L. Pauling, The Nature of the Chemical Bond, Cornell University Press, New York, 1939.
[16] Y. Zhang, Inorg. Chem. 21 (1982) 3886–3889.
[17] S. Benmokhtar, A. El Jazouli, J.P. Chaminade, P. Gravereau, F. Guillen, D. de Waal, J. Solid State Chem. 177 (2004) 4175–4182.
[18] B.F. Mentzen, A. Latrach, J. Appl. Crystallogr. 16 (1983) 430.
[19] B.F. Mentzen, A. Latrach, J. Bouix, A.W. Hewat, Mater. Res. Bull. 19 (1984) 549–554.